Smac mimetic-induced caspase-independent necroptosis requires RIP1 in breast cancer

GONGSHENG JIN[1,2*], YADONG LAN[2*], FUSHENG HAN[2], YIMING SUN[3], ZHE LIU[3], MINGLIANG ZHANG[2], XIANFU LIU[2], XIAOJING ZHANG[2], JIANGUO HU[2], HAO LIU[3] and BENZHONG WANG[1]

[1]Department of Breast Surgery, The First Affiliated Hospital of Anhui Medical University, Hefei, Anhui 230022; [2]Department of Surgical Oncology, The First Affiliated Hospital of Bengbu Medical College, Bengbu, Anhui 233004; [3]Faculty of Pharmacy, Bengbu Medical College, Bengbu, Anhui 233030, P.R. China

Received January 5, 2015; Accepted October 19, 2015

DOI: 10.3892/mmr.2015.4542

Abstract. There is an urgent requirement for the development of novel targeted therapies to treat breast cancer, which is the most comment type of malignancy among women. The evasion of apoptosis is a hallmark of cancer, and is often due to the upregulation of inhibitor of apoptosis proteins (IAPs) in tumor cells. Second mitochondrial-derived activator of caspase/direct IAP-binding protein with low PI is a natural IAP antagonist, which is found in the mitochondrion; this protein has a motif, which binds to a surface groove on the baculovirus IAP repeat domains of the IAPs. In the present study, the effects of the LCL161 Smac mimetic, a small molecule IAP antagonist, on breast cell lines was examined. The results from MTT and colony formation assays demonstrated that LCL161 markedly inhibited the proliferation and induced the apoptosis of MDA-MB-231 and MCF-7 cell lines. As determined by western blotting, cIAP1 was degraded in the breast cancer cells, which occurred in an LCL161-dependent manner. Upon caspase activation, LCL161 treatment induced necroptosis, another form of programmed cell death. The downregulation of receptor-interacting protein kinase-1 via small interfering RNA protected the cells from LCL161-induced necroptosis. Taken together, the results of the present study showed that LCL161 can induce multiple forms of programmed cell death in breast cancer cells, and may thus offer promise as an anticancer agent in diverse genotypic backgrounds.

Correspondence to: Professor Benzhong Wang, Department of Breast Surgery, The First Affiliated Hospital of Anhui Medical University, 218 Jixi Road, Hefei, Anhui 230022, P.R. China
E-mail: wangbenzheong2459@126.com

Professor Hao Liu, Faculty of Pharmacy, Bengbu Medical College, 2600 Donghai Road, Bengbu, Anhui 233030, P.R. China
E-mail: liuhao6886@foxmail.com

*Contributed equally

Key words: second mitochondrial-derived activator of caspase mimetic, LCL161, apoptosis, inhibitor of apoptosis protein, receptor-interacting protein kinase-1, necroptosis

Introduction

Breast cancer, as the most frequently diagnosed type of cancer in women, has become the primary cause of cancer-associated mortality in women worldwide (1). It was estimated that ~1,700,000 new breast cancer cases were diagnosed in 2012, with 6,300,000 cases of breast carcinoma-associated mortality occurring in the same year, according to GLOBOCAN 2012 (1). Furthermore, the incidence and mortality rates of breast cancer have increased by >20 and 14%, respectively, since the 2008 statistics (2). The sharp rise in breast cancer incidence is particularly evident in developing countries (2). These statistics emphasize the requirement for novel and effective breast cancer-targeted therapeutic agents.

The occurrence and development of cancer is a complex process, which ultimately leads to the deregulation of cell signaling pathways that govern cell proliferation and survival (3-5). Over the past two decades, there has been a shift from conventional treatments, including surgery, radiotherapy and chemotherapy, towards more specific targeted therapies (6). Breast cancer is a heterogeneous disease comprising multiple subtypes with different molecular signatures, prognoses and responses to therapies (7). As knowledge of the underlying molecular mechanisms responsible for tumor development and chemotherapeutic resistance has increased, contemporary treatment of breast cancer has entered an era of targeted therapies based on molecular typing, and examples of these molecular targeted therapeutics for breast cancer include tyrosine kinase inhibitors (TKIs), angiogenesis inhibitors and agents that perturb DNA repair (8). In addition, reactivation of the apoptotic program in order to overcome resistance of tumor cells to cell death is being pursued as a novel cancer therapeutic strategy (9,10).

Apoptosis is genetically programmed cell death, which operates via distinct biochemical and genetic pathways; these pathways are also utilized during development and homeostasis in normal tissues (11). Consistent with this, the evasion of apoptosis is denoted as one of the key 'hallmarks' of cancer (4). Apoptotic pathways include the mitochondrial/intrinsic

pathway and the death receptor/extrinsic pathway; and each of these signaling cascades activates caspases, which are the critical effector molecules of apoptosis. The intrinsic apoptotic pathway is initiated by permeabilization of the mitochondria outer membrane, which leads to the activation of caspase 9, whereas the extrinsic pathway is triggered by ligand binding to death receptors, which leads to caspase 8 activation. Subsequently, the activation of effector caspases 3 and/or 7 leads to the cleavage of downstream substrates and the final execution of apoptosis (12,13).

The upregulation of inhibitor of apoptosis proteins (IAPs) is a mechanism by which tumor cells evade apoptosis. IAPs with one or more baculovirus IAP repeat domains belong to a family of key apoptosis regulators and are overexpressed in multiple human malignancies (14); thus, they are relevant targets for therapeutic intervention. In order to execute apoptosis, the activity of IAPs can be inhibited when they are bound to second mitochondria-derived activator of caspase (Smac)/direct IAP-binding protein with low PI (DIABLO), which is released from mitochondria into the cytosol. X-linked IAP (XIAP), cIAP1 and cIAP2, which are three major members of the IAPs family, are all targeted by Smac (15,16).

Another form of programmed cell death, termed 'necroptosis', proceeds via a caspase-independent route. When either caspase 8 or FLICE-like inhibitory protein are absent, or the activation or function of caspase 8 or Fas-associated death domain (FADD) is suppressed, phosphorylated receptor-interacting protein kinase-1 (RIP1), receptor-interacting kinase-3 (RIP3) and mixed lineage kinase domain-like protein assemble into a complex referred to as the 'necrosome' (17-20). However, the mechanisms mediating the execution of necroptosis remain to be fully elucidated. This is a critical gap in current understanding, as necroptosis-associated events are implicated in the pathophysiological processes of several diseases, including myocardial infarction and stroke (21,22), ischemia-reperfusion injury (23,24), atherosclerosis (25) and other common clinical disorders. Thus, an improved knowledge of necroptosis may lead to the identification of necroptosis inhibitors, and thus provide a novel collection of therapeutic agents to modulate this alternate form of cell death.

LCL161 is a small, orally available Smac mimetic compound, which binds to and triggers the degradation of several IAPs; which is then associated with the induction of apoptosis via caspase activation (26). LCL161 was designed to mimic the AVPI tetrapeptide binding motif at the Smac N-terminus, as this region is required for binding to XIAP, cIAP1 and cIAP2. Upon binding to cIAP1, LCL161 triggers the autoubiquitination and proteasomal degradation of cIAP1, which is followed by nuclear factor-κB activation and tumor necrosis factor-α-dependent apoptosis (27). LCL161 also potentiates the anti-leukemic effects of TKIs (28).

The present study was designed to evaluate the effect of LCL161 in human breast cancer cells, and to delineate the molecular mechanisms by which LCL161 causes cell death.

Materials and methods

Reagents and antibodies. The LCL161 Smac mimetic was purchased from Active Biochemicals Co., Ltd. (Hong Kong, China) and dissolved in dimethyl sulfoxide (DMSO; BioSharp, Hefei, China) as a stock solution of 1 mmol·l^{-1}. Rabbit anti-XIAP (cat. no. bs-1281R; 1:500) and rabbit anti-cIAP1 (cat. no. bs-4262R; 1:500) were purchased from Bioss, Inc (Hong Kong, China). Rabbit anti-cIAP2 (cat. no. AP6142a; 1:1,000) was purchased from Abgent, Inc. (Shuzhou, China), and rabbit anti-B-cell lymphoma 2 (Bcl-2)-associated X protein (BAX; cat. no. 50599-2-lg; 1:2,000) and rabbit anti-Bcl-2 (cat. no. 12789-1-AP; 1:1,000) were purchased from Proteintech Group, Inc. (Chicago, IL, USA). Rabbit anti-myeloid cell leukemia (Mcl)-1 (cat. no. sc-819; 1:500) and rabbit anti-RIP1 (cat. no. sc-7881; 1:500) were purchased from Santa Cruz Biotechnology, Inc., (Dallas, TX, USA). Rabbit anti-β-actin (cat. no. BL005A; 1:1,000) was purchased from BioSharp. An Annexin V Fluorescein isothiocyanate (FITC)/propidium iodide (PI) Apoptosis Detection kit was purchased from KeyGen Biotech Co., Ltd. (Nanjing, China).

Cell culture. MDA-MB-231 and MCF-7 human breast cancer cell lines were obtained from Shanghai Cell Bank, (Shanghai, China). The cells were cultivated in Dulbecco's modified Eagle's medium (DMEM; Gibco; Thermo Fisher Scientific, Inc., Waltham, MA, USA) supplemented with 10% fetal bovine serum (Gibco; Thermo Fisher Scientific, Inc.), 44 mmol·l^{-1} sodium bicarbonate, 20 Iu·l-^{1} penicillin, and 20 Iu·l^{-1} streptomycin (North China Pharmaceutical Group Corp., Shijiazhuang, China). The cells were grown at 37.1˚C in a 5% CO_2 humidified atmosphere.

Analysis using a 3-(4,5-dimethyl-2-thiazolyl)-2,5-diphenyl-2H-tetrazolium-bromide (MTT) assay. The breast carcinoma cells were seeded at a density of 7x10^3 cells/well in a 96-well plate for 24 h, and were then treated with increasing doses of LCL161. Following 24, 48 and 72 h of exposure to LCL161, the cells were incubated with 15 μl MTT (5 mg/ml in PBS) per well for 4 h at 37.1˚C. After 4 h, the supernatant was discarded and 150 μl of DMSO was added to each well. The absorbance of the samples at 490 nm was measured on a microplate reader (Synergy HT; BioTek Instruments, Inc., Winooski, VT, USA).

Western blot analysis. The cells were collected and homogenized in radioimmunoprecipitation assay lysis buffer (Roche Diagnostics, Basel, Switzerland) for 0.5 h on ice. Subsequently, the cell lysates were centrifuged at 13,225 x g for 0.5 h at 4˚C to separate the proteins. The proteins were quantified using a Bicinchoninic Acid Protein Assay kit (BioSharp). The proteins (50 μg) were dissociated via 10% SDS-PAGE and subsequently blotted onto polyvinylidene fluoride membranes (EMD Millipore, Billerica, MA, USA) using Rotiphorese SDS-PAGE buffer (Carl Roth, Karlsruhe, Germany). The membranes were blocked with skimmed milk (50 mg·l^{-1}) for 2 h and incubated with the appropriate primary antibody overnight at 4˚C, followed by incubation with conjugated secondary antibodies for 2 h at 20˚C. The proteins were visualized using enhanced chemiluminescence (ECL) reagents (EMD Millipore) and the signals were measured using a Chemidoc XRS imaging system (Universal Hood II; BioRad Laboratories, Inc., Hercules, CA, USA).

Colony formation assays. The cells (5x10^3 MDA-MB-231 cells; 7x10^3 MCF-7 cells) were seeded at the same density in six-well plates for 24 h at 37˚C. The cells were exposed to different

doses of LCL161. Cells were grown for 4 or 6 days at 37˚C, and fixed with ECL reagents at -20˚C for 10 min, following which the colonies were stained with crystal violet (Beyotime Institute of Biotechnology, Shanghai, China). Groups of cells containing >50 cells were identified as a colony under a microscope (CK30; Olympus Corporation, Toyko, Japan).

Mitochondrial transmembrane potential (ΔΨm). The detection of ΔΨm was performed using a fluorescence microscope (IX71; Olympus Corporation) with 5,5',6,6'-tetrachloro-1,1',3,3'-tetraethyl-benzimidazolylcarbocyanine iodide (JC-1; Beyotime Institute of Biotechnology) staining. Briefly, following drug treatment, the cells were incubated with 10 μmol·l^{-1} JC-1 for 30 min at 37˚C in the dark. Images of the cells were then captured using the IX71 Olympus microscope.

Annexin V-FITC/PI apoptosis assay. Cellular apoptosis analysis was performed using an Annexin V-FITC Apoptosis Detection kit (KeyGen Biotech Co., Ltd.). The cells ($2x10^5$) were plated in a six-well plate and treated with LCL161 for 24 h. The cells were harvested and collected by low-speed centrifugation at 110.2 x g for 5 min at 25˚C (LD5-2A; Beijing Lab Centrifuge Co., Ltd., Beijing, China) and resuspended in 500 ml ice-cold binding buffer. Subsequently, the cells were incubated with 5 μl Annexin V-FITC and PI for 15 min at room temperature in the dark, following which analysis was performed using an Accuri C6 flow cytometer (BD Biosciences).

Electron microscopic detection. The cells from the various treatment groups were fixed with 3% glutaraldehyde and 2% paraformaldehyde in 0.1 M PBS buffer (pH 7.4) for 0.5 h, postfixed with 1% osmium tetroxide for 1.5 h, and washed and stained in 3% aqueous uranyl acetate for 1 h. The samples were then dehydrated in an ascending series of ethanol and acetone, and embedded in Araldite. Ultrathin sections were cut on a Reichert ultramicrotome, double-stained with 0.3% lead citrate, and examined under a JEM-1230 electron microscope (JEOL, Ltd., Tokyo, Japan).

Small interfering (si)RNA. The breast cancer cells were seeded at a density of $2x10^5$ cells/well in six-well plates and allowed to reach ~50% confluence on the day of transfection. A negative control RNA construct (5'-UUCUCCGAACGUGUCACG UTT-3') and siRNA against RIP1 (5'-CCUUCUGAGCAG CUUGAUUTT-3') were synthesized by Shanghai GenePharma Co., Ltd. (Shanghai, China). The cells were transfected with 20 nmol·l^{-1} siRNA in Opti-MEM medium (Invitrogen; Thermo Fisher Scientific, Inc.) using Lipofectamine 2000 reagent (Invitrogen; Thermo Fisher Scientific, Inc.). The efficiency of siRNA knockdown was assessed using western blot analysis 24 h following transfection.

Statistical analysis. The data are expressed as the mean ± standard error of the mean from triplicate assays, and differences between treatment groups were determined using two-tailed Student's *t*-test. Statistical analysis was performed using Prism 5.0 software (GraphPad Prism, Inc., La Jolla, CA, USA). P<0.05 was considered to indicate a statistically significant difference.

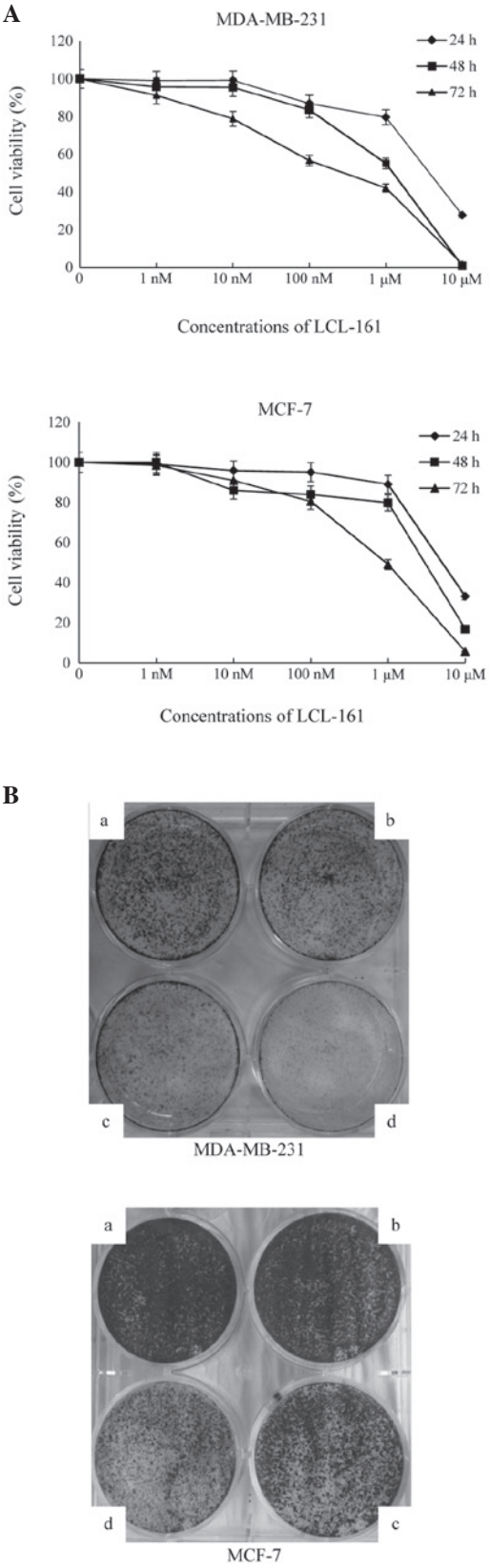

Figure 1. LCL161 inhibits the proliferation of breast cancer cells. (A) MDA-MB-231 and MCF-7 cells were cultured with various concentrations of LCL-161 (1, 10 and 100 nmol·l^{-1}, 1 and 10 μmol·l^{-1}) for 24, 48 and 72 h, following which cell viability was analyzed using a 3-(4,5-dimethyl-2-thiazolyl)-2,5-diphenyl-2H-tetrazolium bromide assay. Data are presented as the mean ± standard error of the mean from three independent experiments. (B) MDA-MB-231 cells were treated with control, 2.5, 5 or 10 nmol·l^{-1} for 4 days, and MCF-7 cells were treated with control, 10, 20 and 40 nmol·l^{-1} for 6 days. Colonies were stained with crystal violet. Images are representative of three independent experiments.

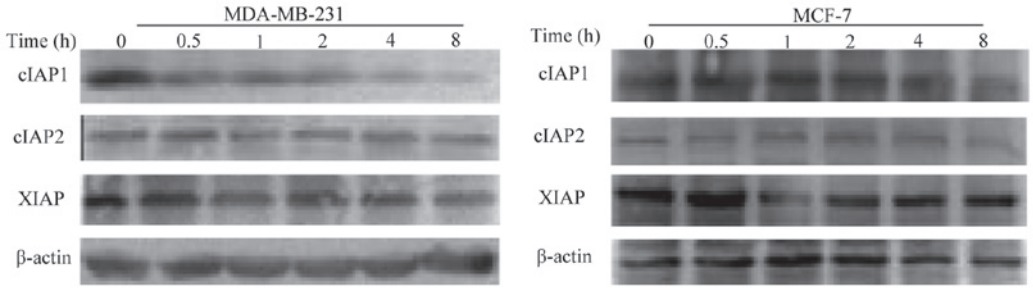

Figure 2. LCL161 induces cell death by the degradation of cIAP1 in breast cancer cell lines. The MDA-MB-231 and MCF-7 cells treated with 1 μmol·l^{-1} LCL161 for different durations and subjected to western blot analysis. β-actin was used as a loading control. The blots shown are representative of three independent experiments. cIAP1, cellular inhibitor of apoptosis protein 1; XIAP, X-linked IAP.

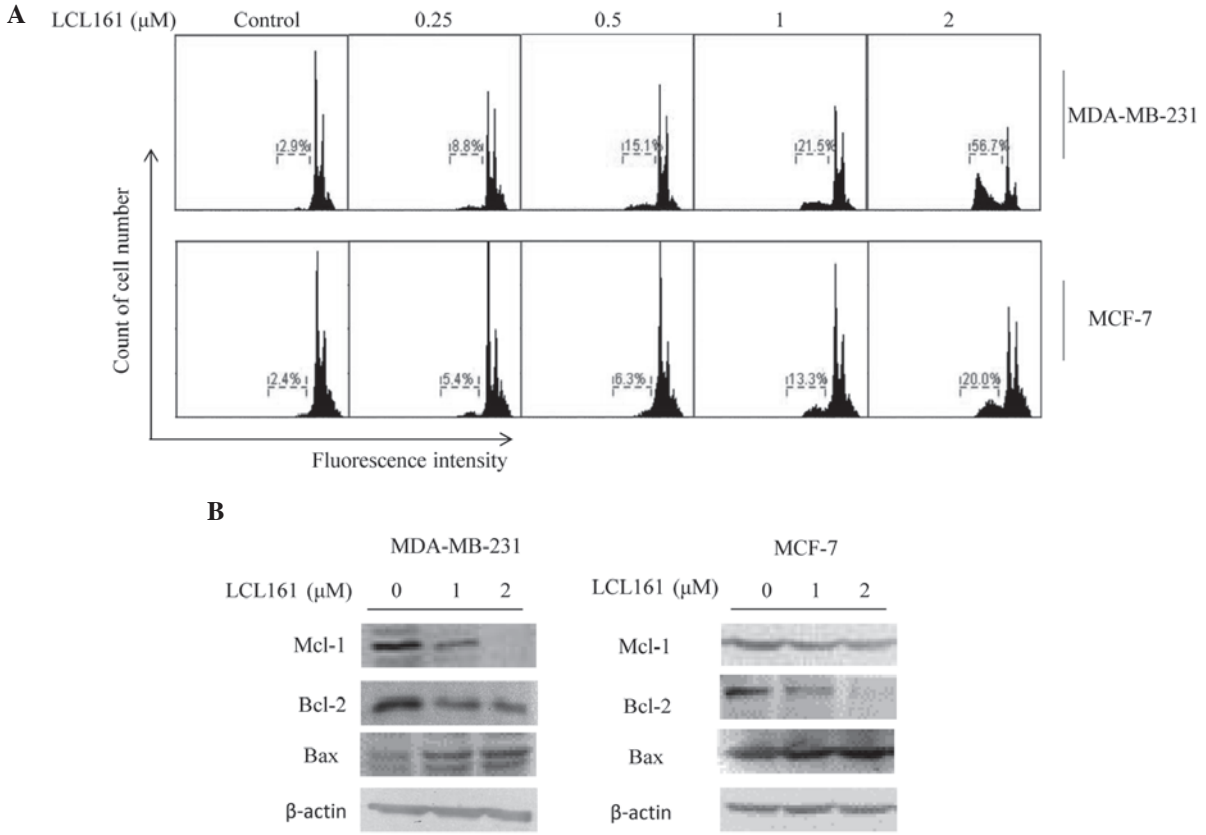

Figure 3. LCL161 induces apoptosis in breast cancer cell lines. (A) MDA-MB-231 and MCF-7 cells were treated with various concentrations of LCL161 for 24 h. The detection of apoptosis was performed by flow cytometry using propidium iodide staining; percentages represent the total percentage of apoptotic cells. The results are representative of three independent experiments. (B) Whole-cell lysates from the MDA-MB-231 and MCF-7 cells treated with different concentrations of LCL161 were subjected to western blot analysis. The blots are representative of three independent experiments. Mcl-1; myeloid cell leukemia-1; Bcl-2, B cell lymphoma-2; Bax, Bcl-2-associated X protein.

Results

LCL161 inhibits the proliferation of breast cancer cells. In order to determine the antitumor effect of LCL161 on breast cancer cells, the present study performed an MTT assay 24, 48 and 72 h following exposure of the cells to LCL161. As shown in Fig. 1A, cell viability was inversely proportional to the duration of exposure and the concentration of LCL161 in the MDA-MB-231 and MCF-7 cells. When the concentration of drug was increased (a to d), the number of cell colonies was reduced. Colony outgrowth assays performed following treatment with lower half maximal inhibitory concentrations in the two cell lines also confirmed the inhibitory effects of LCL161 on cell proliferation (Fig. 1B).

LCL161 causes cell death via the degradation of cIAP1 in breast cancer cells. To investigate whether modulation of IAPs occurred following treatment with LCL161, the present study examined the expression levels of the three major members of the IAPs family, XIAP, cIAP1 and cIAP2, in the breast cancer cells. The results revealed that the levels of cIAP1 were reduced in the two cell lines, however, the effect was more marked in the MDA-MB-231. LCL161 caused a marginal reduction in the levels of XIAP, and had almost no effect on

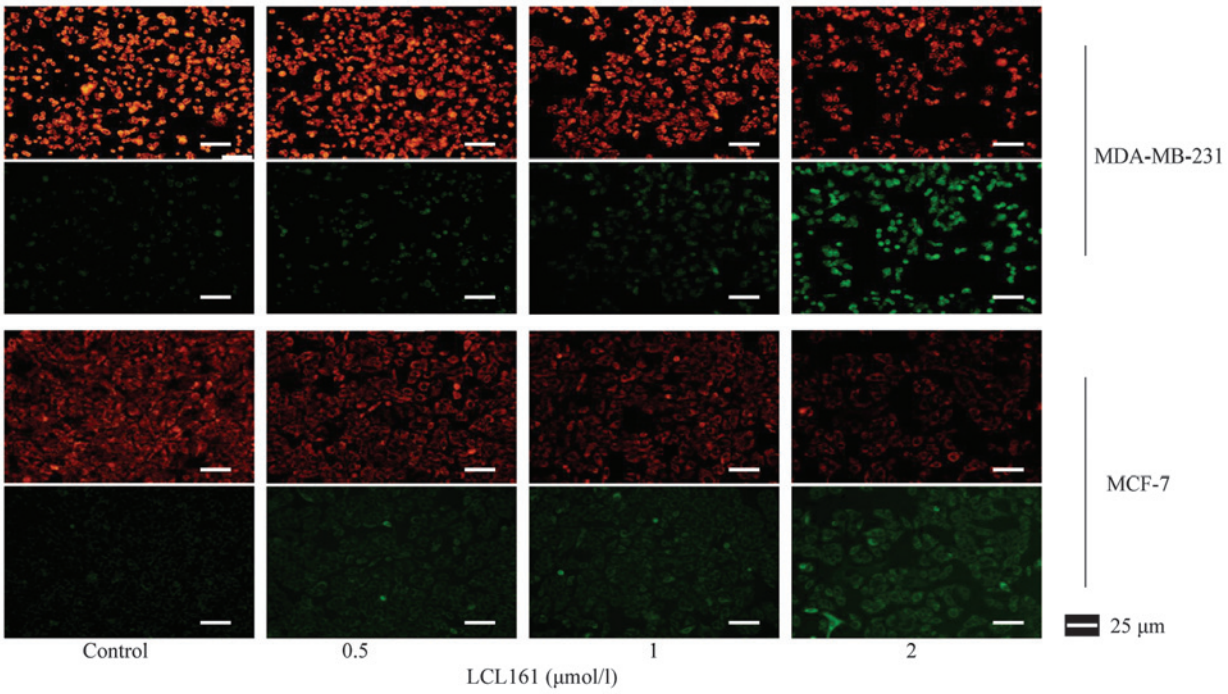

Figure 4. LCL-161 reduces the ΔΨm of breast cancer cells. The MDA-MB-231 and MCF-7 cells treated with various concentrations of LCL161 for 24 h, following which they were subjected to measurement of ΔΨm using 5,5',6,6'-tetrachloro-1,1',3,3'-tetraethyl-benzimidazolylcarbocyanine iodide staining. Red fluorescence represents the JC-1 complex, green fluorescence represents the JC-1 monomer. The images are representative of three independent experiments. ΔΨm, mitochondrial membrane potential.

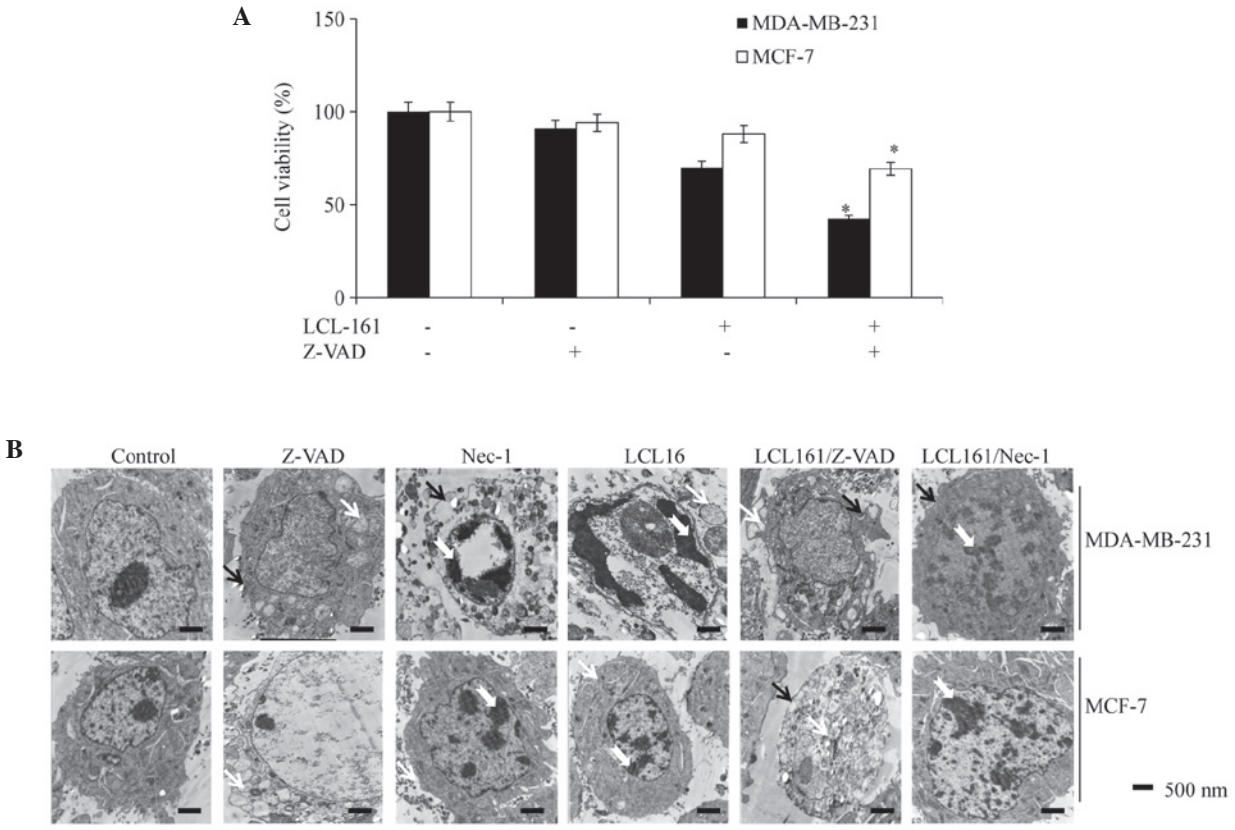

Figure 5. LCL-161+*pan*-caspase inhibitor enhances cell death. (A) Viability of MDA-MB-231 or MCF-7 cells treated with DMSO, LCL161 (1 μmol·l^{-1}) and LCL161/z-VAD (20 μmol·l^{-1}) were analyzed using a 3-(4,5-dimethyl-2-thiazolyl)-2,5-diphenyl-2H-tetrazolium bromide assay. Data are representative of three independent experiments and are expressed as the mean ± standard error of the mean (*P<0.05, vs. the LCL161 group). (B) MDA-MB-231 and MCF-7 cells were treated with DMSO, z-VAD, Nec-1, LCL161, LCL161+z-VAD or LCL161+Nec-1 and were analyzed by electron microscopy. White arrowheads indicate the swelling of cellular organelles in the cells treated with z-VAD or LCL161+z-VAD; black arrowheads indicate cell membrane integrity in the cells treated with DMSO, Nec-1, LCL161 or LCL161+Nec-1, and membrane breakdown in the cells treated with z-VAD or LCL161+z-VAD. Dovetail arrowheads indicate pyknosis and clotted chromatin. DMSO, dimethyl sulfoxide; Nec-1; necrostatin-1.

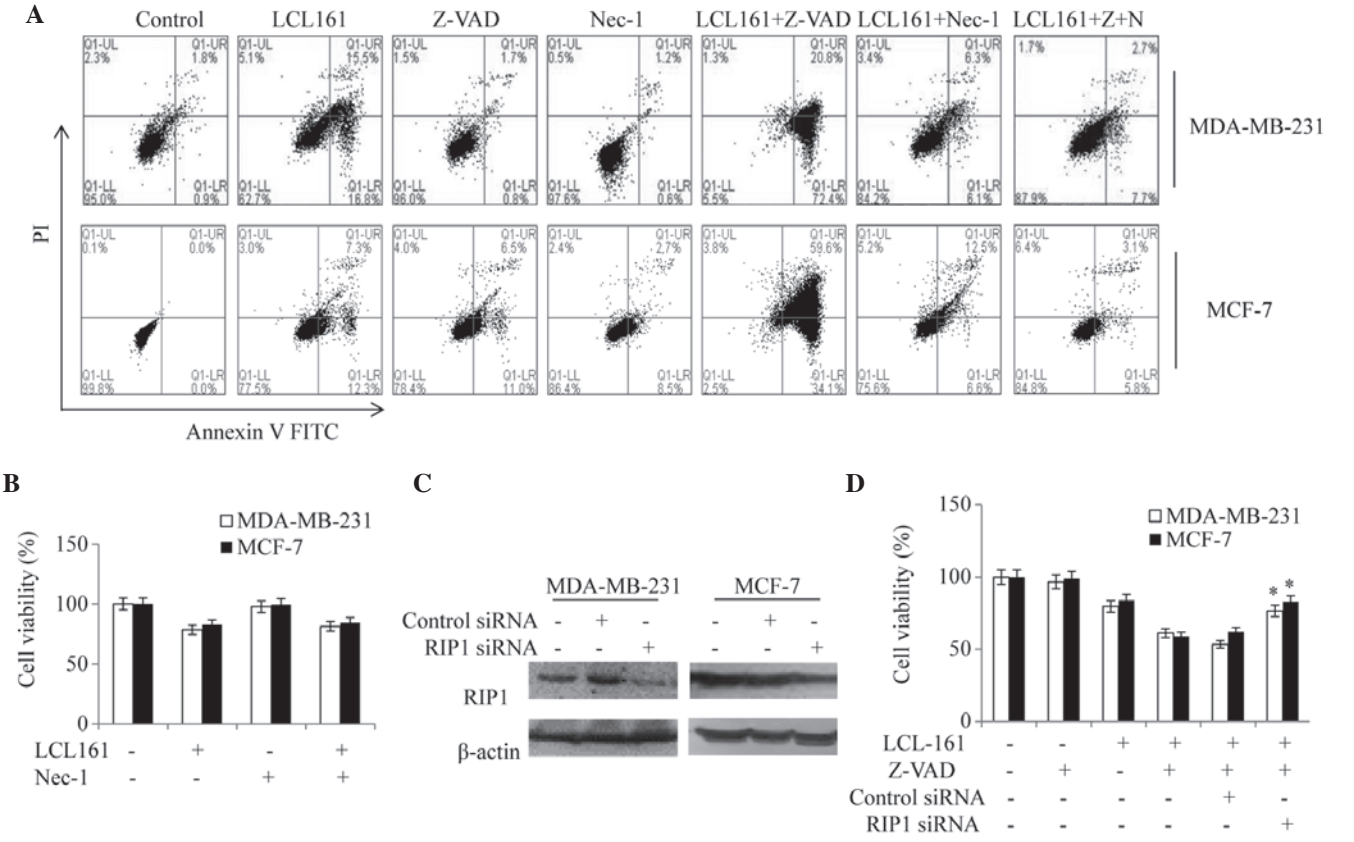

Figure 6. Cell death induced by LCL161+z-VAD-fmk depends on RIP1. (A) MDA-MB-231 and MCF-7 cells treated with DMSO, z-VAD, Nec-1, LCL161, LCL161+z-VAD, and LCL161+Nec-1 for 24 h were analyzed using an Annexin V-FITC/PI apoptosis assay. (B) MDA-MB-231 and MCF-7 cells treated with DMSO, LCL161, Nec-1 and LCL161+Nec-1 for 24 h were analyzed using a 3-(4,5-dimethyl-2-thiazolyl)-2,5-diphenyl-2H-tetrazolium bromide assay. (C) MDA-MB-231 and MCF-7 cells were transfected with control or RIP1 siRNA and, after 48 h, whole-cell lysates were subjected to western blot analysis. (D) MDA-MB-231 and MCF7 cells were transfected with RIP1 siRNA, cultured for 24 h and then treated with LCL161 or LCL161+z-VAD. Data are representative of three independent experiments and are expressed as the mean ± standard error of the mean (*P<0.05, vs. the LCL161+Z-VAD group). RIP1, receptor-interacting protein kinas-1; DMSO, dimethyl sulfoxide; Nec-1; necrostatin-1; FITC, fluorescein isothiocyanate; PI, propidium iodide; siRNA, small interfering RNA; UR, upper right (late apoptotic cells); UL, upper left (cell debris); LL, lower left (normal cells); LR, lower right (early apoptotic cells).

the levels of cIAP2 (Fig. 2). These results indicated that the LCL161-dependent inhibition of proliferation was associated with the degradation of cIAP1.

LCL161 induces apoptosis in breast cancer cell lines. Flow cytometric analysis revealed that, in the MDA-MB-231 cells, LCL161 induced apoptosis in a dose-dependent manner, in which levels increased between 2.9 and 56.7%. Consistent with the results of the MTT assay, the level of apoptosis in the MCF-7 cells was lower, increasing between 2.4 and 20.0% (Fig. 3A). The present study also examined the levels of several other apoptosis-associated proteins. Among these, the expression levels of Mcl-1 and Bcl-2 were downregulated following 24 h treatment with LCL161, whereas the expression of BAX increased (Fig. 3B).

Fluorescence microscopy of the JC-1 stained cells revealed that LCL161 reduced the $\Delta\Psi m$, as there was a reduction in the red/green ratio due to the loss of red fluorescent J aggregates (Fig. 4). It was concluded from these data that LCL161 effectively inhibited cell proliferation, owing to its ability to activate the apoptotic pathway.

LCL161 in combination with pan-caspase inhibitor induces necroptosis. To examine whether LCL161-induced apoptosis was caspase-dependent, the MDA-MB-231 and MCF-7 cells were treated separately with LCL161 in combination with Z-VAD-fmk, a cell permeable *pan*-caspase inhibitor. As shown in Fig. 5A, Z-VAD-fmk treatment exacerbated LCL161-dependent cell death. To further characterize this caspase-independent cell death, cell morphology was examined using transmission electron microscopy (TEM). As shown in Fig. 5B, in the breast cancer cells treated with DMSO, Z-VAD or the Nec-1 RIP1 inhibitor, the majority of cells exhibited a normal 'viable' morphology, which included intact cytoplasmic membranes. By contrast, treatment with LCL161 alone induced cell death with classical apoptotic morphology. Under the microscope, the chromatin was pyknotic and clotted, and vacuolization due to the fusion of the endoplasmic reticulum and plasma membrane appeared in the cytoplasm. The cytoplasmic membranes were intact. By contrast, in the cells treated with the Smac mimetic and Z-VAD in combination, the mitochondria were swollen and cytoplasmic membranes were discontinuous; which are hallmarks of necrosis. Thus, the form of cell death induced by LCL161 in the absence of classical apoptosis appears to proceed via a type of necrosis. In the cells treated with the combination of LCL161 and the specific RIP1 inhibitor, Nec-1, the major form of cell death was consistent with the cells treated with LCL161 alone under TEM.

Cell death induced by the combination of LCL161 and Z-VAD-fmk is dependent on RIP1. An Annexin V-FITC/PI apoptosis assay was used to detect the levels of apoptosis induced by LCL161 with Z-VAD and/or Nec-1 on the MDA-MB-231 and MCF-7 cells. The results revealed that the apoptotic rate decreased in the LCL161/Z-VAD group, however, Nec-1 inhibited this increase, resulting in a lower apoptotic rate, compared with the LCL161-only group (Fig. 6A). In addition, the results demonstrated that the viability of the MDA-MB-231 cells following treatment with Nec-1 and LCL161 was similar to that following LCL161 treatment alone (81 and 78%, respectively; Fig. 6B) These results suggested that LCL161+Z-VAD-induced necroptosis was regulated by Nec-1.

The present study also examined whether specific ablation of the expression of RIP1 by siRNA phenocopied the effect of the RIP1 inhibitor. Notably, the downregulation of RIP1 protected the cells, compared with the cells treated with LCL161 alone (Fig. 6C and D), confirming that necroptosis induced by the combination of LCL161 and Z-VAD-fmk was dependent on RIP1.

Discussion

Clinically, breast cancer can be divided into three major subclasses: Luminal A/B subtype, HER-2-amplified subtype, and basal-like subtype (7). Treatment with trastuzumab, an anti-HER2 monoclonal antibody, improves the overall survival rate of patients with HER2-positive breast cancer in adjuvant and first-line settings (29). However, no therapy has demonstrated such efficacy in the treatment of the other two breast cancer subtypes. Thus, the present study selected two breast carcinoma lines of the non HER-2-amplified subtype in order to evaluate the efficacy of the Smac mimetic, LCL161.

The results of the present demonstrated that the Smac mimetic, LCL161, induced apoptosis and inhibited the proliferation of the breast cancer cell lines. Apoptosis is a strictly regulated process, and its misregulation is involved in several human diseases, including cancer (30). As key regulators of apoptosis, IAPs bind to and inhibit key caspases, thus conferring resistance to several treatment regimens (31,32). LCL161 is a newly designed orally bioavailable monovalent mimetic of Smac, which has advanced in clinical development. It was designed to mimic the AVPI tetrapeptide binding motif of Smac, therefore, it can interact with XIAP, cIAP1 and cIAP2 (33). Oral administration of LCL161 inhibits tumor growth in a mouse model of multiple myeloma (34). In breast carcinoma cells, the reduction of cIAP1 following exposure to LCL161 may be due to the binding of LCL161 to cIAP1. The binding leads to a conformational change of cIAP1, stimulating RING domain-dependent homodimerization, which results in cIAP1 auto-ubiquitination and subsequent rapid proteasomal degradation. Upon loss of cIAP1, the non-ubiquitinated form of RIP1, together with FADD and caspase-8 form a complex that activates caspase-8 and triggers the extrinsic pathway of apoptosis (34).

Bcl-2 family protein members are indispensable for the correct function of major organ systems, and mutations affecting their levels or activity are correlated with cancer (35). These proteins are either pro-apoptotic, including BAX and Bcl-2 antagonist/killer 1 (BAK), or anti-apoptotic, including Bcl-2, Mcl-1, Bcl-extra large (XL) and Bcl-W). The activity of these proteins ultimately converges on the mitochondrial outer membrane, and an excess of pro-apoptotic activity triggers mitochondrial membrane permeabilization and caspase activation (36). There is extensive crosstalk between the mitochondrial and death receptor-mediated death pathway. For example, BH3-interacting-domain death agonist (BID), a pro-apoptotic Bcl-2 member, which is processed to truncated BID (tBID) by the activity of caspase-8. tBID translocates to the mitochondrial membrane, where it binds to BAX and BAK, and stimulates the release of cytochrome *c*, leading to activation of the intrinsic pathway (37). By contrast, anti-apoptotic MCL-1 is integral in cell survival and apoptosis (38,39). The present study assessed the effects of LCL161 on Mcl-1, BAX and BAK. The compound reduced the level of Mcl-1, and concomitantly increased the levels of BAX and BAK, aggravating the mitochondrial pathway of apoptosis.

However, the present study also observed a caspase-independent, RIP1-dependent, type of necrotic cell death in response to LCL161. This indicates another example of necroptosis, which occurs when caspases are inhibited or when apoptosis cannot be activated efficiently. Since cIAP1 is an E3 ubiquitin ligase (40,41), its loss upon LCL161 treatment leads to the accumulation, or reduced ubiquitination, of cIAP substrates, which may include RIP1, a known target of XIAP and cIAPs (42). Thus, the present study hypothesized that LCL161-dependent degradation of cIAP1 leads to the accumulation of active RIP1, which in turn triggers formation of the necrosome and cell death.

In conclusion, the findings of the present study suggested that LCL161 may be suitable for application as a targeted therapeutic for the treatment of patients with breast cancer. Future investigations are requireded to determine the efficacy and therapeutic index of LCL161 *in vivo*.

Acknowledgements

This study was supported by the National Natural Science Foundation of China (grant no. 81372899). The authors would like to thank Editage/Cactus for assistance with English language editing.

References

1. Ferlay J, Soerjomataram I, Dikshit R, Eser S, Mathers C, Rebelo M, Parkin DM, Forman D and Bray F: Cancer incidence and mortality worldwide: Sources, methods and major patterns in GLOBOCAN 2012. Int J Cancer 136: E359-E386, 2015.
2. Bray F, Ren JS, Masuyer E and Ferlay J: Global estimates of cancer prevalence for 27 sites in the adult population in 2008. Int J Cancer 132: 1133-1145, 2013.
3. Fearon ER and Vogelstein B: A genetic model for colorectal tumorigenesis. Cell 61: 759-767, 1990.
4. Hanahan D and Weinberg RA: Hallmarks of cancer: The next generation. Cell 144: 646-674, 2011.
5. Sherr CJ: Cancer cell cycles. Science 274: 1672-1677, 1996.
6. Higgins MJ and Baselga J: Targeted therapies for breast cancer. J Clin Invest 121: 3797-3803, 2011.
7. Sørlie T, Perou CM, Tibshirani R, Aas T, Geisler S, Johnsen H, Hastie T, Eisen MB, van de Rijn M, Jeffrey SS, *et al*: Gene expression patterns of breast carcinomas distinguish tumor subclasses with clinical implications. Proc Natl Acad Sci USA 98: 10869-10874, 2001.
8. Bourdeanu L and Luu T: Targeted therapies in breast cancer: Implications for advanced oncology practice. J Adv Pract Oncol 5: 246-260, 2014.

9. Reed JC: Apoptosis-based therapies. Nat Rev Drug Discov 1: 111-121, 2002.
10. Johnstone RW, Ruefli AA and Lowe SW: Apoptosis: A link between cancer genetics and chemotherapy. Cell 108: 153-164, 2002.
11. Lockshin RA and Williams CM: Programmed cell Death-I. Cytology of degeneration in the intersegmental muscles of the pernyi silkmoth. J Insect Physiol 11: 123-133, 1965.
12. Fulda S and Debatin KM: Extrinsic versus intrinsic apoptosis pathways in anticancer chemotherapy. Oncogene 25: 4798-4811, 2006.
13. Bai L, Smith DC and Wang S: Small-molecule SMAC mimetics as new cancer therapeutics. Pharmacol Ther 144: 82-95, 2014.
14. Dubrez L, Berthelet J and Glorian V: IAP proteins as targets for drug development in oncology. Onco Targets Ther 9: 1285-1304, 2013.
15. Du C, Fang M, Li Y, Li L and Wang X: Smac, a mitochondrial protein that promotes cytochrome *c*-dependent caspase activation by eliminating IAP inhibition. Cell 102: 33-42, 2000.
16. Salvesen GS and Duckett CS: IAP proteins: Blocking the road to death's door. Nat Rev Mol Cell Biol 3: 401-410, 2002.
17. Li J, McQuade T, Siemer AB, Napetschnig J, Moriwaki K, Hsiao YS, Damko E, Moquin D, Walz T, McDermott A, *et al*: The RIP1/RIP3 necrosome forms a functional amyloid signaling complex required for programmed necrosis. Cell 150: 339-350, 2012.
18. Holler N, Zaru R, Micheau O, Thome M, Attinger A, Valitutti S, Bodmer JL, Schneider P, Seed B and Tschopp J: Fas triggers an alternative, caspase-8-independent cell death pathway using the kinase RIP as effector molecule. Nat Immunol 1: 489-495, 2000.
19. Zhang DW, Shao J, Lin J, Zhang N, Lu BJ, Lin SC, Dong MQ and Han J: RIP3, an energy metabolism regulator that switches TNF-induced cell death from apoptosis to necrosis. Science 325: 332-336, 2009.
20. Sun L, Wang H, Wang Z, He S, Chen S, Liao D, Wang L, Yan J, Liu W, Lei X and Wang X: Mixed lineage kinase domain-like protein mediates necrosis signaling downstream of RIP3 kinase. Cell 148: 213-227, 2012.
21. Degterev A, Hitomi J, Germscheid M, Ch'en IL, Korkina O, Teng X, Abbott D, Cuny GD, Yuan C, Wagner G, *et al*: Identification of RIP1 kinase as a specific cellular target of necrostatins. Nat Chem Biol 4: 313-321, 2008.
22. Smith CC, Davidson SM, Lim SY, Simpkin JC, Hothersall JS and Yellon DM: Necrostatin: A potentially novel cardioprotective agent? Cardiovasc Drugs Ther 21: 227-233, 2007.
23. Linkermann A, Bräsen JH, Himmerkus N, Liu S, Huber TB, Kunzendorf U and Krautwald S: Rip1 (receptor-interacting protein kinase 1) mediates necroptosis and contributes to renal ischemia/reperfusion injury. Kidney Int 81: 751-761, 2012.
24. Oerlemans MI, Liu J, Arslan F, den Ouden K, van Middelaar BJ, Doevendans PA and Sluijter JP: Inhibition of RIP1-dependent necrosis prevents adverse cardiac remodeling after myocardial ischemia-reperfusion in vivo. Basic Res Cardiol 107: 270, 2012.
25. Lin J, Li H, Yang M, Ren J, Huang Z, Han F, Huang J, Ma J, Zhang D, Zhang Z, *et al*: A role of RIP3-mediated macrophage necrosis in atherosclerosis development. Cell Rep 3: 200-210, 2013.
26. Chen KF, Lin JP, Shiau CW, Tai WT, Liu CY, Yu HC, Chen PJ and Cheng AL: Inhibition of Bcl-2 improves effect of LCL161, a SMAC mimetic, in hepatocellular carcinoma cells. Biochem Pharmacol 84: 268-277, 2012.
27. Varfolomeev E, Blankenship JW, Wayson SM, Fedorova AV, Kayagaki N, Garg P, Zobel K, Dynek JN, Elliott LO, Wallweber HJ, *et al*: IAP antagonists induce autoubiquitination of c-IAPs, NF-kappaB activation and TNFalpha-dependent apoptosis. Cell 131: 669-681, 2007.
28. Weisberg E, Ray A, Barrett R, Nelson E, Christie AL, Porter D, Straub C, Zawel L, Daley JF, Lazo-Kallanian S, *et al*: Smac mimetics: Implications for enhancement of targeted therapies in Leukemia. Leukemia 24: 2100-2109, 2010.
29. Marty M, Cognetti F, Maraninchi D, Snyder R, Mauriac L, Tubiana-Hulin M, Chan S, Grimes D, Antón A, Lluch A, *et al*: Randomized phase II trial of the efficacy and safety of trastuzumab combined with docetaxel in patients with human epidermal growth factor receptor 2-positive metastatic breast cancer administered as first-line treatment: The M77001 study group. J Clin Oncol 23: 4265-4274, 2005.
30. Lowe SW and Lin AW: Apoptosis in cancer. Carcinogenesis 21: 485-495, 2000.
31. Wang S, Bai L, Lu J, Liu L, Yang CY and Sun H: Targeting inhibitors of apoptosis proteins (IAP) for new breast cancer therapeutics. J Mammary Gland Biol Neoplasia 17: 217-228, 2012.
32. Hassan M, Watari H, AbuAlmaaty A, Ohba Y and Sakuragi N: Apoptosis and molecular targeting therapy in cancer. Biomed Res Int 2014: 150845, 2014.
33. Wu G, Chai J, Suber TL, Wu JW, Du C, Wang X and Shi Y: Structural basis of IAP recognition by Smac/DIABLO. Nature 408: 1008-1012, 2000.
34. Chauhan D, Neri P, Velankar M, Podar K, Hideshima T, Fulciniti M, Tassone P, Raje N, Mitsiades C, Mitsiades N, *et al*: Targeting mitochondrial factor Smac/DIABLO as therapy for multiple myeloma (MM). Blood 109: 1220-1227, 2007.
35. Adams JM and Cory S: The Bcl-2 protein family: Arbiters of cell survival. Science 281: 1322-1326, 1998.
36. Kvanskul M and Hinds MG: Structural biology of the Bcl-2 family and its mimicry by viral proteins. Cell Death Dis 4: e909, 2013.
37. Kim BM and Chung HW: Desferrioxamine (DFX) induces apoptosis through the p38-caspase8-Bid-Bax pathway in PHA-stimulated human lymphocytes. Toxicol Appl Pharmacol 228: 24-31, 2008.
38. Kozopas KM, Yang T, Buchan HL, Zhou P and Craig RW: MCL1, a gene expressed in programmed myeloid cell differentiation, has sequence similarity to BCL2. Proc Natl Acad Sci USA 90: 3516-3520, 1993.
39. Sano M, Hayashi E, Murakami H, Kishimoto H, Fukuzawa R and Nemoto N: Mcl-1, an anti-apoptotic Bcl-2 family member, essentially overlaps with insulin-producing cells in neonatal nesidioblastosis. Virchows Arch 452: 469-470, 2008.
40. Gyrd-Hansen M, Darding M, Miasari M, Santoro MM, Zender L, Xue W, Tenev T, da Fonseca PC, Zvelebil M, Bujnicki JM, *et al*: IAPs contain an evolutionarily conserved ubiquitin-binding domain that regulates NF-kappaB as well as cell survival and oncogenesis. Nat Cell Biol 10: 1309-1317, 2008.
41. Vaux DL and Silke J: IAPs, RINGs and ubiquitylation. Nat Rev Mol Cell Biol 6: 287-297, 2005.
42. Park SM, Yoon JB and Lee TH: Receptor interacting protein is ubiquitinated by cellular inhibitor of apoptosis proteins (c-IAP1 and c-IAP2) in vitro. FEBS Lett 566: 151-156, 2004.